

# Exponential Elastic Model and Its Application in Real-Time Simulation

Hualiang Zhong and Terry M. Peters  
Imaging Research Laboratories, Robarts Research Institute  
100 Perth Drive, London, ON, Canada, N6A 5K8  
{hzhong, tpeters}@imaging.robarts.ca

## ABSTRACT

The development of accurate material models and computational methods are two fundamental components in building a real-time realistic surgery simulator. In this paper, we use a least-squares method to calibrate an exponential model of pig liver based on the assumption of incompressible material under a uniaxial testing mode. With the obtained parameters, the stress-strain curves generated from the least-squares approach are compared to those from the corresponding model built in ABAQUS and to experimental data, resulting in mean deviations of 1.9% and 4.8%, respectively. Furthermore we demonstrate equivalence between the parameters of the exponential material model and those of linear or other nonlinear models under small strains. Finally, we incorporate this calibrated exponential model into a nonlinear finite element framework to simulate the behavior of liver during an interventional procedure, and achieve real-time performance through use of an interpolation approach.

**Keywords:** SIM, Image-Guided Surgery, Enhanced Reality

## I. INTRODUCTION

Computer-aided surgical simulation systems have great potential in medical education and image-guided procedures. Since the integration of incorrect material properties into deformable tissue models may give rise to unrealistic tissue behavior during a simulation, further investigation of tissue biomechanical parameters, development of more efficient and accurate computer algorithms, and validation of simulated deformations against real in vivo data must be addressed [1;2]. While for surgical planning or image-guided procedures, simulation needs to emphasize an accurate description of tissue's response to an interventional action, modeling or implementing such a system has been proved to be difficult due to the requirements of both speed and accuracy [3]. Unlike classical engineering material, soft tissues do not have a linear stress-strain relation (i.e. they do not obey Hooke's law), so their mechanical properties cannot be easily characterized by a small number of elastic constants [1]. Noting this nonlinearity, many attempts have been made to derive mathematical models of soft tissue behavior based on a strain energy function, often defined in terms of three principle variables,  $I_1 = C_{kk}$ ,  $I_2 = (I_1^2 - C_{kl}C_{lk})$ ,  $I_3 = \det C_{kl} = J^2$  where  $C_{ij}$  is an entry in the right Cauchy-Green strain tensor [4-6]. The typical example of this approach is the Mooney-Rivlin law which was used to model tissues such liver [7] or breast [8] in static analysis, and the work of Wu [9] who employed it in real time surgical simulation. However this model is more suitable for modeling rubber-like materials or soft tissue under small strains [7;8;10], rather than those with large-scale deformations encountered in a surgical procedure. Therefore to develop a nonlinear FE solver we have employed an exponential strain energy function [10]:

$$W_{\text{exp}}(I_1, J) = C_s (e^{b(I_1 - 3)} - 1), \quad (1)$$

which was first proposed by Blatz *et al.* and Demiray (see [10]). Demiray assumed that biological materials were elastic, homogenous, isotropic and incompressible, and that the exponential constitutive law was a function of only the axial Green-Lagrange strain components.

The goal of this project is to build a simulation system to model a pig liver's respiratory cycle, verifiable with a magnetic tracking device. The accuracy of such a system relies on an appropriate elastic model and its accurately calibrated parameters. These parameters can usually be obtained with different trial and error approaches, based on a computation model built from FEM software packages such as ABAQUS® (ABAQUS, Inc., Providence, RI), to fit experimental data [7;8;11]. However, if the model involves large-scale deformations in its boundary conditions, the

finite element approach often has difficulty in converging. To address this problem occurring in validating the results of surgery simulation, Kerdok et al [12] designed a “truth cube” to establish physical standards for soft tissue modeling, instead of using FE modeling methods. Usually calibrating nonlinear material models involves large strain deformations, and finding appropriate elastic parameters for these models requires testing a broad range of values. These present the iterative finite-element optimization approach with serious challenges in both numeric convergence and computational time.

In this paper, we use a least-squares method to calculate the parameters of the exponential model, based on the experimental local effective modulus (LEM) obtained in [7] for pig liver tissue, and then incorporate this model into a real-time finite element based simulation system [13].

## II. CALIBRATION OF EXPONENTIAL CONSTITUTIVE MODEL

The mechanical properties of pig liver have been recently addressed in many papers. Ottensmeyer [14] measured pig liver during a minimally invasive surgical procedure and estimated the Young’s modulus (YM) to be around 10~15 Kpa. A similar experiment on pig liver from Kim [15] yielded 3Kpa for YM when a semi-infinite medium was assumed. While these YMs provide a reference to the characterization of pig liver under small strains, they are not sufficient for characterizing large deformations. Cater et al [16] conducted ex vivo experiments on pig liver and analyzed their data using the exponential model (1). In their analysis, they imposed the uniaxial test assumption on their indentation test and obtained the results of  $b = 0.08$  and  $bC_s = 0.06$ . They estimated YM to be about 4.9 Mpa which is very high comparing to other studies. In this paper, we apply the uniaxial assumption on a uniaxial experimental dataset tested in an ex vivo experiment by Hu and Desai [7] for pig liver tissue at large strains. Based on their experimental results, we calibrate the exponential model and then incorporate the model into a surgical simulation environment.

Due to vascular redistribution and interstitial fluid, soft tissue is slightly compressible, so the exponential model (1) is often penalized by a bulk term  $W_b = -\int_1^{I_3} P(I_3)dI_3$ . For example, Pathmanathan *et al.* [17] assumed that  $P(I_3) = p/2$  for simulating a large deformation of a breast. The coefficient  $p$  in the bulk term serves as a Lagrange multiplier, which can be interpreted as a hydrostatic pressure. In our later simulation, we extend (1) by adding the bulk term  $W_b$  with  $P(I_3) = -C_b \ln(I_3)$ , to obtain

$$W(I_1, J) = C_s (e^{b(I_1-3)} - 2b \ln J - 1) + C_b (2J^2 \ln J - J^2 + 1). \quad (2)$$

Models of this nature are used extensively in the modeling of various organs such as kidney [18], breast [17] and heart [19]. While we choose  $C_b$  to be 100Kpa in the simulation of nearly isochoric behavior under a typical physiological stress [10], in this section, we concentrate on the evaluation of the parameters  $C_s$  and  $b$  based on the local effective modulus (LEM) in [7] and the following theoretical model.

### 2.1 Local Effective Modulus

Since no model can exactly match the experimental results in a large range of strains, Hu and Desai expressed their experimental results in [7] through the LEM, defined as  $E^{(i)} = \frac{\sigma_i - \sigma_{i-1}}{\epsilon_i - \epsilon_{i-1}}$ ,  $i = 1, 2, \dots, n$ , where  $n$  is the number of

intervals partitioning the whole strain domain. Consequently the LEM in the whole domain can be fitted with a polynomial in the term of displacement  $x$ . Two of their samples have been expressed in the following polynomials:

$$\begin{aligned} E_1 &= 0.019 - 0.016x + 0.012x^2 - 0.00082x^3 + 0.0016x^4 \\ E_2 &= 0.014 - 0.012x + 0.0098x^2 - 0.0009x^3 + 0.0014x^4 \end{aligned} \quad (3)$$

From the definition of LEM we may write the Cauchy stress  $\sigma = \int E(\epsilon_u) \Delta \epsilon_u$  where  $\epsilon_u = -\ln \lambda_u$  as defined in [7]. The relation between the strain and the displacement can be obtained from the experimental configuration in [7], where we know  $\lambda_u = 1 - x/10$ . Therefore we have  $d\epsilon_u = dx/(10 - x)$  and  $x = 10(1 - e^{-\epsilon_u})$ . Consequently the integration of (3) generates the experimental relations between the stress and displacement for the two samples:

$$\begin{aligned}\sigma_1 &= 0.0019x - 0.000705x^2 + 0.000353x^3 - 0.000006x^4 + 0.0000125x^5 \\ \sigma_2 &= 0.0014x + 0.00001x^2 + 0.000327x^3 + 0.000002x^4 + 0.0000282x^5\end{aligned}\quad (4)$$

where the constant terms from the above integral are set to be zero by assuming that their initial stresses are null.

In Hooke's law, the ratio of stress and strain is assumed to be constant. However, for liver tissue with large strains (30%), if we combine (4) with (3), we may generate the following experimental relations:

$$\begin{aligned}E &= \frac{d\sigma}{d\varepsilon} = 253\sigma^2(\varepsilon) - 12.3\sigma(\varepsilon) \\ E &= \frac{d\sigma}{d\varepsilon} = 63.6\sigma^2(\varepsilon) - 6.4\sigma(\varepsilon)\end{aligned}\quad (5)$$

From Figure 1, it can be seen that the expressions (3) and (5) could closely match each other, but unlike LEM which is a polynomial function of displacement  $x$ , (5) is independent of the displacement or the details of the model's configuration, and therefore may serve as an appropriate description of elasticity.

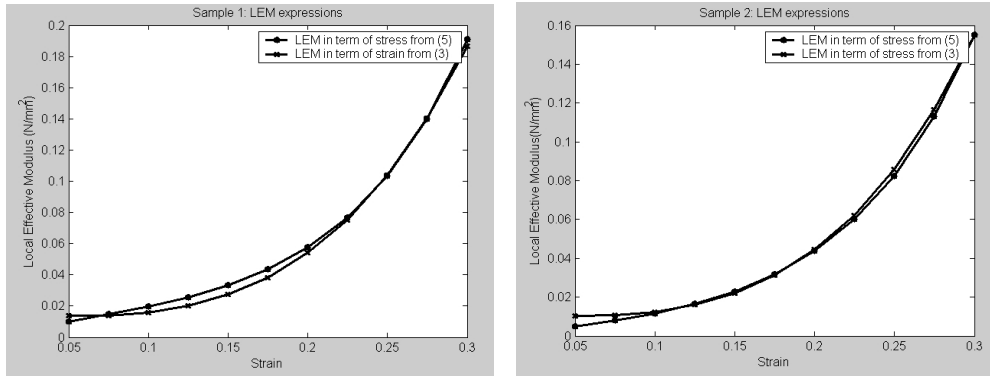


Figure 1: The local effective moduli derived from (3) and (5) for sample 1 (left) and for sample 2 (right).

Generally if  $\sigma$  satisfies the expression  $\frac{d\sigma}{d\varepsilon} = a_2\sigma^2(\varepsilon) + a_1\sigma(\varepsilon)$ , then we may generate

$$\sigma = \frac{a_1\omega_0 \exp(a_1\varepsilon)}{\{a_2\sigma_0 + a_1 - a_2\omega_0 \exp(a_1\varepsilon)\}}, \quad \omega_0 = \sigma_0 \exp(-a_1\varepsilon_0)$$

where  $\sigma_0$  and  $\varepsilon_0$  are initial stress and initial strain, respectively, with  $\sigma_0 > 0$ . Similar to the Hooke's law, the above expression describes the elastic property through an explicit function but is also applicable to large scale deformations.

## 2.2 Evaluation of the Shear Modulus

We first consider expression (1), which satisfies the incompressible condition. In a uniaxial deformation mode, we assume that the principle stretches satisfy:

$$\lambda_1 = \lambda_u, \quad \lambda_2 = \lambda_3 = \frac{1}{\sqrt{\lambda_u}}.$$

Then from the principle of virtual work, we have  $\delta W = (\delta\lambda_u)T$ , where  $T$  is the uniaxial nominal stress. It follows that

$$T = \frac{\partial W}{\partial \lambda_u} = 2(\lambda_u - \lambda_u^{-2}) \frac{\partial W}{\partial I_1}.\quad (6)$$

After the substitution of the above energy function  $W$  with (1), the expression (6) can be written as:

$$T = 2C_s b(e^{-\varepsilon_u} - e^{2\varepsilon_u}) \exp\{b(e^{-2\varepsilon_u} + 2e^{\varepsilon_u} - 3)\}.\quad (7)$$

Suppose  $\sigma_i$  is as defined in (4), then the corresponding nominal stress  $T_i = N(\sigma_i) = \frac{\Delta_0}{\Delta} \sigma_i$ , where  $\Delta_0$  is the initial contact area and  $\Delta$  is the current area obtained from  $\epsilon_u$  and the incompressible property. Consequently, with  $T$  defined in (7), the equation  $T=T_i$  can be written as

$$C_s b \exp\{b(e^{-2\epsilon_u} + 2e^{\epsilon_u} - 3)\} = \frac{N(\sigma_i)}{2(e^{-\epsilon_u} - e^{2\epsilon_u})}. \quad (8)$$

Replacing  $x$  in (4) with  $x=10(e^{-\epsilon_u}+1)$  and then taking the natural logarithmic of each side of (8), we obtain

$$A + BH(\epsilon_u) = S_j(\epsilon_u)$$

where  $A = \ln(C_s b)$ ,  $B = b$ ,  $H(\epsilon_u) = e^{-2\epsilon_u} + 2e^{\epsilon_u} - 3$ , and  $S_j(\epsilon_u) = \ln N(\sigma_j(\epsilon_u)) - \ln\{2(e^{-\epsilon_u} - e^{2\epsilon_u})\}$ . With the sampled values of the logarithmic strain  $\epsilon_u^j = -\ln(1 - x^j/10)$ , we obtain the matrix equation:

$$\begin{pmatrix} 1 & H(\epsilon_u^{(1)}) \\ \dots & \dots \\ 1 & H(\epsilon_u^{(m)}) \end{pmatrix} \begin{pmatrix} A \\ B \end{pmatrix} = \begin{pmatrix} S_j(\epsilon_u^{(1)}) \\ \dots \\ S_j(\epsilon_u^{(m)}) \end{pmatrix}. \quad (9)$$

Applying a least-squares method to solve (9), we obtain the unknowns  $A$  and  $B$ , and consequently the parameters  $C_s$  and  $b$  as follows.

	b	Cs (MPa)	E (MPa)
Sample 1	1.81	0.0013	0.0139
Sample 2	3.54	0.000678	0.0144

Table 1: Parameters of an exponential model for two samples of pig liver fitted with 24 sampling values under strain 30%.

	b	Cs (MPa)	E (MPa)
Sample 1	1.73	0.0014	0.0142
Sample 2	3.60	0.000664	0.0143

Table 2: Parameters of an exponential model for two samples of pig liver fitted with 48 sampling values under strain 30%.

Substituting the parameters  $C_s$  and  $b$  into theoretical formula (7) with their calculated values in Table 1, we obtain the nominal stress/strain relations of the two samples and they are compared with the experimental stress/strain curves (Figure 2):

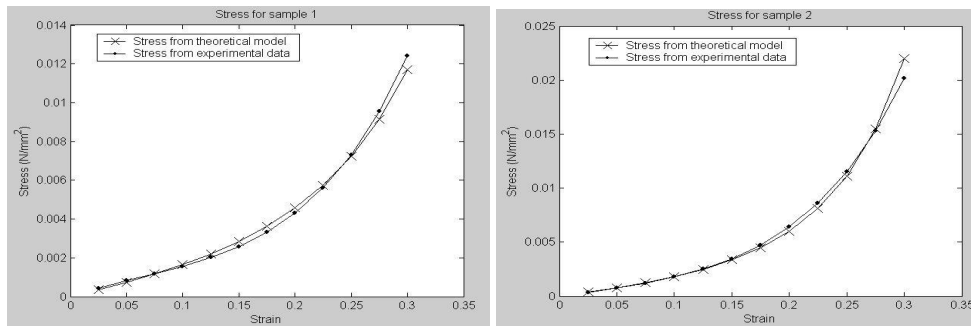


Figure 2: Left: The nominal stress of sample 1 in (7) vs. the derived experimental curve  $N(\sigma_1)$  in (4); Right: The nominal stress of sample 2 in (7) vs. the derived experimental curve  $N(\sigma_2)$  in (4).

### 2.3 Validation of Parameters with FEM Approach

Considering that the compression experiments in [7] were performed on a cube of  $10 \times 10 \times 10 \text{mm}^3$ , we next build a corresponding computational model using the FEM package ABAQUS to validate the exponential constitutive law and the above parameters. We follow the approach described in [7] by building a deformable plane stress model in ABAQUS to simulate the uniaxial test. The element type was CPS4 (4-node bilinear plane stress) with the model consisting of 100 elements. A set of values for the vertical displacements of the top plane is prescribed and there is no

friction on either the top or bottom surfaces, so that they may slide freely. Since exponential forms are not default material formats in ABAQUS, we created a UHYPER subroutine to evaluate equation (1).

We now insert the parameters generated from the least-squares method into these ABAQUS computational models and then compare their results with those from the derived experimental expression (4). Based on the two sample data sets, their comparisons are very close to Figure 2. Instead of illustrating the difference between the results of ABAQUS and (4), Figure 3 demonstrates the similarity between the ABAQUS and the theoretic assumption (7). The latter has been compared with (4) in Figure 2. It should be mentioned that the stresses obtained from ABAQUS are Cauchy stress, which need to be converted into nominal stress for coincidence with Figure 2.

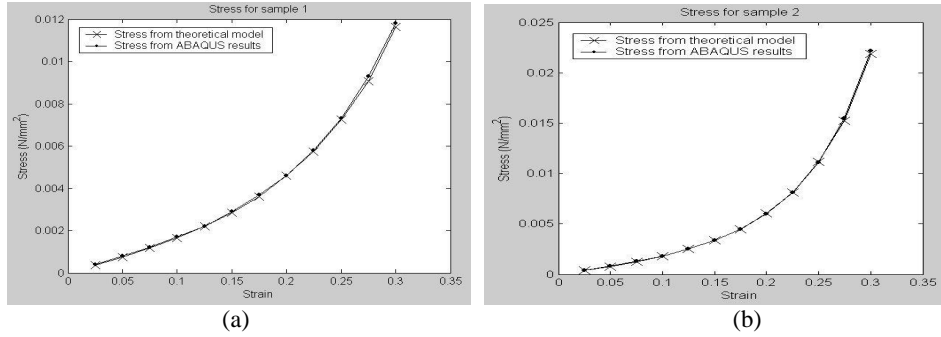


Figure 3: The nominal stress/strain relations in (7) vs. those from ABAQUS: (a) for sample 1 and (b) for sample 2.

#### 2.4 Equivalence in Different Models

While there are various elastic models often used in describing nonlinear elasticity, these calibrated nonlinear models should be comparable to YM under small strains. So it is worth comparing the parameters in Table 1 with those of other constitutive models. For the exponential model (1) we may deduce from (7) that  $\sigma = 6C_s b \varepsilon_u + o(\varepsilon_u)$ . From [20] we know  $\sigma = 6(C_{10} + C_{01})\varepsilon_u + o(\varepsilon_u)$  for the Mooney-Rivlin model and  $\sigma = 3\left(\sum_{i=1}^N \mu_i\right)\varepsilon_u + o(\varepsilon_u)$  for the Ogden model. It follows that under a small strain, we have

$$C_s b \approx C_{10} + C_{01} \approx \frac{1}{2} \left( \sum_{i=1}^N \mu_i \right) \approx \frac{E}{6}. \quad (10)$$

The Young's moduli in Table 1 for a small-scale deformation can therefore be obtained from  $E = 6C_s b$ . Conversely the value of  $C_s b$  (but not  $C_s$  or  $b$  independently) may be derived from the parameters of the Ogden model or a Young's modulus  $E$ . The latter may be calibrated through some experiments with small strain. With the equivalence (10), the derived YM obtained from the samples of liver tissues are around 14 Kpa (see Table 1).

As shown in [7], the Ogden model was used to approximate the experimental result for a sample of the pig liver under a large-scale deformation (30%). Using this model, the calibrated parameters are  $\mu_1 = -0.179$ ,  $\mu_2 = 0.177$ ,  $\mu_3 = 0.007$ ,  $\sum_{i=1}^3 \mu_i = 0.005$ . Consequently we substitute these values into (10) and obtain the results  $C_s b = 0.0025$ ,  $E = 0.015$ , which are very close to our own (i.e.  $C_s b = 0.0024$ ,  $E = 0.0144$ ) in Table 1. While the YM derived from the parameters of the nonlinear model are slightly different from those calibrated directly under small strains, due to the changes of the approximation domain, they are still comparable to 15Kpa, an value obtained in in-vivo testing by Ottensmeyer [14] and Samur [1] respectively, and 9Kpa for a lamb liver by Shi et al [21]

For the exponential model, while  $C_s b$  may be determined by the initial stress-strain relation and while different liver samples may share a similar value of  $C_s b$ , each  $C_s$  or  $b$  could be quiet different in the large range of the strain domain. This explains why the exponential model is capable of precisely expressing various stress-strain relations.

### III. REAL-TIME SIMULATION

In the last section, we calibrated the elastic relation between the stress and strain. As mentioned in [16], while the elastic property obtained from experimental measurements is important for modeling tissue deformation, combining this property with a real time simulator remains a challenge. In the absence of rapid computation, the value of these calibrated models is limited. So in the remainder of this section, we focus on the method of achieving a real-time speed with the exponential model. Considering the compressibility of soft tissue for more accurate results, we adopted the strain energy function (2) as an elastic model in the following simulation.

Minimizing the general energy function  $\Pi := \int_{\Omega} W(\mathbf{E})dV - \Pi_{ext}$ , with the problem domain partitioned into a set of tetrahedral elements in which we interpolate the internal points through the natural shape basis functions  $N_i(\zeta, \eta, \xi)$  defined in the local coordinate system  $\zeta(\zeta, \eta, \xi)$  [13], we obtain

$$\int_{\omega} \mathbf{B}^T \boldsymbol{\sigma} dV - \mathbf{f}_{ext} = \mathbf{0}, \quad (11)$$

where the strain-displacement matrix  $\mathbf{B}$  is a constant matrix if  $N_i(\zeta, \eta, \xi)$  is linear [12]. Since the Cauchy stress  $\boldsymbol{\sigma}_{ij}$  satisfies  $\boldsymbol{\sigma}_{ij} = \frac{\partial W}{\partial b_{ij}}$ , where  $b_{ij}$  is an left Cauchy-Green strain tensor [22], we can compute that

$$\boldsymbol{\sigma}_{ij} = \frac{2}{J} C_s b \exp\{b(I_1 - 3)\} b_{ij} + 2(-C_s b + pJ^2 \ln(J)) \delta_{ij},$$

where  $\delta_{ij}$  is the Kronecker delta function. We take the parameters  $C_s=0.678(\text{KPa})$ ,  $b=3.54$  from the sample 2, and  $C_b=100\text{KPa}$  as suggested in [10]. Specifying the invariants  $I_1$  and  $J$  in the current coordinates and then integrating equation (11) over all the elements, we obtain a set of non-linear algebraic equations

$$\boldsymbol{\Phi}(\mathbf{U}) = \mathbf{f}_{ext}(\mathbf{U}) - \mathbf{P}(\mathbf{U}) = \mathbf{0}. \quad (12)$$

To solve this equation, a Newton-Raphson method is employed. It has been shown that solving such a system often suffers from excessive computation time and divergence. To address these problems specifically in our simulation, we adopt the following preprocessing approach.

Suppose that a needle contacts the surface of the pig liver at a given node  $s$ , then using Newton's iterative method combined with the conjugate gradient algorithm, we obtain the displacement of each free node  $p$ . If we assume the displacement at  $p$  is a function  $Q_p$  of the movement of the needle tip under a given configuration, this function can be approximated via an interpolation approach.

To approximate the function  $Q_p$ , we choose a basis  $\{1, X_j\}_{j=1, \dots, k}$  so that each displacement  $d_p$  can be expressed as

$$d_p \cong \tilde{Q}_p(X_j) = a_0 + \sum_{j=1}^k a_j X_j. \quad (13)$$

Now with the FEM solver, we generate  $N$  sets of displacements for each free node based on the  $N$  given sets  $\{\delta x_s^i, \delta y_s^i, \delta z_s^i\}$  of displacements of the needle tip  $s$ . Suppose that the basis  $\{1, X_j\}_{j=1, \dots, k}$  is equal to  $\{1, \delta x_s, \delta y_s, \delta z_s, \delta x_s \delta y_s, \delta y_s \delta z_s, \delta z_s \delta x_s, (\delta x_s)^2, (\delta y_s)^2, (\delta z_s)^2\}$ , then the coefficients  $a_i$  can be optimized through the over-determined system:

$$S \begin{pmatrix} a_0 \\ a_1 \\ \dots \\ a_9 \end{pmatrix} := \begin{pmatrix} 1 & X_1^1 & X_2^1 & \dots & X_9^1 \\ 1 & X_1^2 & X_2^2 & \dots & X_9^2 \\ \dots & \dots & \dots & \dots & \dots \\ 1 & X_1^N & X_2^N & \dots & X_9^N \end{pmatrix} \begin{pmatrix} a_0 \\ a_1 \\ \dots \\ a_9 \end{pmatrix} = \begin{pmatrix} \delta x_p^1 \\ \delta x_p^2 \\ \dots \\ \delta x_p^N \end{pmatrix}, \quad (14)$$

where  $X_j^v$  is the value of  $X_j$  at  $vR/N$ ,  $v=1, \dots, N$ , and  $R$  is the maximal displacement of the needle tip. This system can be easily solved at a preprocessing stage by

$$(a_0 \ a_1 \ \dots \ a_9)^T = (S^T S)^{-1} S^T (\delta x_p^1 \ \delta x_p^2 \ \dots \ \delta x_p^N)^T. \quad (15)$$

With the obtained coefficients  $a_i$  and the given configuration, we may predict the deformation of a pig liver as the needle's position is changed.

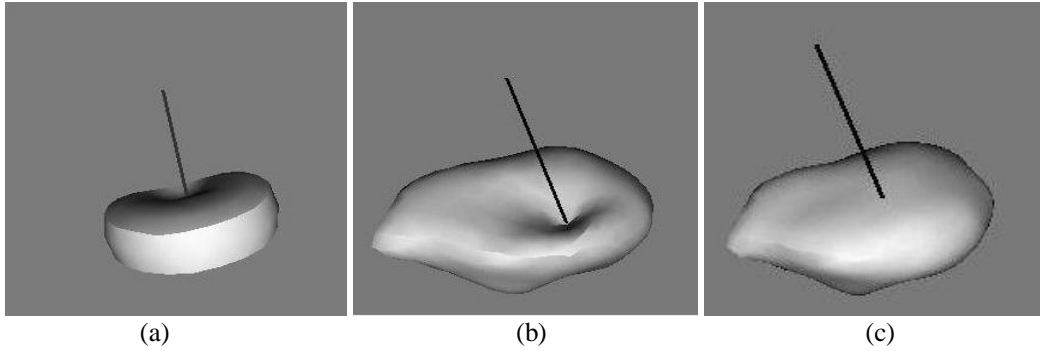


Figure 4. A large-scale deformation effect using the exponential material model on (a) a cylinder, (b) a pig liver and (c) its undeformed shape.

#### IV. DISCUSSION

Recognizing that incorporating inappropriate models or parameters into a surgery simulator could lead to an incorrect or inappropriate behavior of the simulated procedure, in this paper, we choose an exponential model to characterize liver tissue and calibrated its two parameters using the least-squares method (LSM). Compared to the trial and error approach, which usually requires a comprehensive finite element software package, LSM is simple and can be easily incorporated into a surgery simulator. As an indirect calibration approach, this method relies on the theoretical assumptions of material properties (homogenous, isotropic and incompressible) as well as the uniaxial experimental configuration. However, it can achieve an accuracy comparable to that of ABAQUS.

The theoretical model (7) is calibrated from the experimental data and the two results match each other with a maximum error of 4.8% (Figure 2). However, this error can be reduced if we use a higher order exponential elastic law instead of (1). We are also interested in whether the parameters generated by the least-squares method will allow ABAQUS to produce an expected deformation. Figure 3 shows that both the nominal stress/strain curves (7) and those generated by ABAQUS fit very well (with mean a error <1.9%) for the two samples with strains of up to 30%. These results are comparable to the ABAQUS-calibrated Ogden models reported in [7].

In general, the obtained parameters for the two samples of the pig liver are comparable to those for other tissues. For example, for passive canine myocardium, Hunter *et al.* (see [10]) assumed  $b=5.1$  and for kidney, Farshad *et al.* [18] obtained  $b=6.8$  and  $C_s=2.5$  KPa, almost seven times stiffer than the liver we simulated here, but is a realistic reflection of the different mechanical properties of these two organs.

This work is based on the experimental data from uniaxial compression tests in [7], so we only calibrated the incompressible model. For more accurate results relating to volumetric changes, triaxial compression tests may be required. However, in the real time simulation, we penalized the exponential model with a bulk term whose a constant coefficient was suggested in [10]. Also, even though we have demonstrated that the experimental stress/strain relation (4) generated from the LEM expressions of [7] works in this paper, it is still better to employ the stress-strain relations directly from experimental data to avoid introducing unnecessary errors. For example, the initial stress in (4) is assumed to be zero, which could be less than its actual value. Consequently the YM calibrated here may be slightly overestimated.

#### V. CONCLUSIONS

The analytical approach combined with a least-squares method is simple and stable for calibrating a large-scale deformation of soft tissue, and it avoids computational difficulties often encountered in trial and error procedures, which use a comprehensive FEM package for the nonlinear 2D/3D analysis of large-scale deformations. Using this method, we obtained a set of parameters for the two samples of pig liver, and demonstrated that with the calibrated parameters of the exponential form, the results from the ABAQUS computational models closely match the experimental data. This indicates that by using the calibrated exponential model in a simulation, we can achieve an accuracy compatible to the Ogden model characterized by a FEM approach in [7].

We incorporated the exponential material model into our nonlinear FEM solver, modified a surgical simulation system, and achieved a real time execution and the expected visual results. The high fidelity of the exponential constitutive model makes it a potential material format for developing a target tracking or surgery simulation system.

### ACKNOWLEDGEMENTS

The authors gratefully acknowledge the financial support provided by the Canadian Institutes for Health Research MOP 14735, Canadian Foundation for Innovation, and the Ontario Research and Development Challenge Fund.

### Bibliography

- [1] Samur, E., Sedef, M., Basdogan, C., Avtan, L., and Duzgun, O. A robotic indenter for minimally invasive characterization of soft tissues. International Congress Series 1281 (2005), 713-718. 2005. Elsevier.
- [2] Delingette, H., "Toward realistic soft-tissue modeling in medical simulation," *Proc.IEEE*, vol. 86, pp. 512-523, 1998.
- [3] Zhong, H., Wachowiak, M. P., and Peters, T. M. Adaptive finite element technique for cutting in surgical simulation. Proc.SPIE Medical Imaging, Vol.5744. 2005.
- [4] Demiray, H., "A note on the elasticity of soft biological tissues," *J of Biomechanics*, vol. 5 pp. 309-311, 1972.
- [5] Fung, Y. C. Elasticity of soft tissues in simple elongation. Am. J. Physiol. 213, pp.1532-1544, 1967.
- [6] Ogden, R. W., *Non-linear elastic deformations* New York: Ellis Horwood, 1984.
- [7] Hu, T. and Desai, J. Characterization of soft-tissue material properties: large deformation analysis. Medical Simulation: International Symposium. ISMS 2004, pp.28-37. Cambridge, MA, USA, 2004.
- [8] Samani, A. and Plewes, D., "A method to measure the hyperelastic parameters of ex vivo breast tissue samples," *Physics in Medicine and Biology*, vol. 49, pp.4395-4405, 2004.
- [9] Wu, X., Goktekin, T., and Tendrick, F. Adaptive nonlinear finite elements for deformable body simulation using dynamic progressive meshes. Proc. Eurographics2001, pp.349-358. 2001.
- [10] Usyk, T. P. and McCulloch, A., "Computational Methods for Soft Tissue Biomechanics," in Holzapfel, G. A. and Ogden, R. W. (eds.) *Biomechanics of soft tissue in cardiovascular systems* New York: Springer-Verlag, 2003, pp. 273-341.
- [11] Liu, Y., Kerdok, A. E., and Howe, R. D. A nonlinear finite element model of soft tissue indentation. pp.67-76. 2004. Cambridge, MA, Springer-Verlag.
- [12] Kerdok, A. E., Cotin, S. M., Ottensmeyer, M. P., Galea, A. M., Howe, R. D., and Dawson, S. L., "Truth cube: establishing physical standards for soft tissue simulation," *Medical Image Analysis*, vol. 7, no. 3, pp.283-291, 2003.
- [13] Zhong, H., Wachowiak, M. P., and Peters, T. M., "A real time finite element based tissue simulation method incorporating nonlinear elastic behavior," *Computer Methods in Biomechanics and Biomedical Engineering*, vol. 8, no. 3, pp.177-189, 2005.

- [14] Ottensmeyer, M. P., "Minimally invasive instrument for in vivo measurement of solid organ mechanical impedance." Ph.D Thesis Department of Mechanical Engineering, MIT, 2001.
- [15] Kim, J., "Virtual environments for medical training: graphical and haptic simulation of tool-tissue interactions." Ph.D Thesis Department of Mechanical Engineering, MIT, 2003.
- [16] Carter, F. J., Frank, T. G., Davis, P. J., McLean, D., and Cuschieri, A., "Measurements and modelling of the compliance of human and porcine organs," *MED IMAGE ANAL*, vol. 5, pp.231-236, 2001.
- [17] Pathmanathan, P., Gavaghan, D., Whiteley, J., Brady, M., Nash, M., Nielsen, P., and Rajagopal, V. Predicting tumour location by simulating large deformations of the breast using a 3D finite element model and nonlinear elasticity. In Christian, B Haynor D. R. and Hellier P. Eds. Proc. MICCAI2004, LNCS3217, pp.217-224, 2004. Springer-Verlag.
- [18] Farshad, M., Barbezat, M., Flueler, P., Schmidlin, F., Graber, P., and Niederer, P. Material characterization of the pig kidney in relation with the biomechanical analysis of renal trauma. *J of Biomechanics*, vol. 32, no. 4, pp.417-425, 1999.
- [19] Lin, I.-E. and Taber, L. A. Mechanical effects of looping in the embryonic chick heart. *J of Biomechanics* vol. 27, no. 3, pp.311-321, 1994.
- [20] ABAQUS. Analysis User's Manual, version 6.4. ABAQUS, Inc.
- [21] Shi, H. and Farag, A. Validating linear elastic and linear viscoelastic models of lamb liver tissue using cone-beam CT. *International Congress Series* 1281 (2005), pp.473-478, Elsevier, 2005.
- [22] Zienkiewicz, O. C. and Taylor, R. L., *The finite element method, Volume 2: Solid Mechanics* Barcelona, Spain: Butterworth Heinemann, 2000.